Loss of endogenous Nfatc1 reduces the rate of DMBA/TPA-induced skin tumorigenesis

Jill Goldstein[a], Eve Roth[a], Natalie Roberts[a], Rachel Zwick[a], Samantha Lin[a], Sean Fletcher[a], Ana Tadeu[a], Christine Wu[a], Amanda Beck[b], Caroline Zeiss[b], Mayte Suárez-Fariñas[c], and Valerie Horsley[a,d]

[a]Department of Molecular, Cell and Developmental Biology, [b]Department of Comparative Medicine, and [d]Department of Dermatology, Yale University, New Haven, CT 06520; [c]Departments of Population Health Science and Policy, Genetics and Genomics Science, and Dermatology, Icahn School of Medicine, New York, NY 10029

ABSTRACT **Immunosuppressive therapies using calcineurin inhibitors, such as cyclosporine A, are associated with a higher incidence of squamous cell carcinoma formation in mice and humans. Calcineurin is believed to suppress tumorigenesis in part through Nfatc1, a transcription factor expressed primarily in hair follicle bulge stem cells in mice. However, mice overexpressing a constitutively active Nfatc1 isoform in the skin epithelium developed increased spontaneous skin squamous cell carcinomas. Because follicular stem cells can contribute to skin tumorigenesis, whether the endogenous expression of Nfatc1 inhibits or enhances skin tumorigenesis is unclear. Here we show that loss of the endogenous expression of *Nfatc1* suppresses the rate of DMBA/TPA-induced skin tumorigenesis. Inducible deletion of *Nfatc1* in follicular stem cells before tumor initiation significantly reduces the rate of tumorigenesis and the contribution of follicular stem cells to skin tumors. We find that skin tumors from mice lacking *Nfatc1* display reduced *Hras* codon 61 mutations. Furthermore, Nfatc1 enhances the expression of genes involved in DMBA metabolism and increases DMBA-induced DNA damage in keratinocytes. Together these data implicate Nfatc1 in the regulation of skin stem cell–initiated tumorigenesis via the regulation of DMBA metabolism.**

Monitoring Editor
Yukiko Yamashita
University of Michigan

Received: May 15, 2015
Revised: Aug 4, 2015
Accepted: Aug 18, 2015

INTRODUCTION

Stem cells reside within tissues to govern organ homeostasis and regeneration through the coordinated regulation of proliferation and differentiation. When these processes go awry, stem cells can contribute to diseases such as cancer. Indeed, tissue-resident stem cells can initiate tumorigenesis in the mammary gland, intestine, and skin (Barker *et al.*, 2009; Lapouge *et al.*, 2011; Visvader, 2011; White *et al.*, 2011), and cancer stem cells can maintain tumor growth in the epidermis (Schober and Fuchs, 2011; Driessens *et al.*, 2012; Boumahdi *et al.*, 2014). However, the mechanisms controlling the contribution of stem cells to tumors remain largely unknown.

The skin provides an excellent model to explore stem cell function during tumorigenesis. Follicular stem cells are slow-cycling cells that reside within the bulge compartment, express the cell surface marker CD34, and become activated to regenerate the hair follicle during the native hair cycle (Cotsarelis *et al.*, 1990; Blanpain *et al.*, 2004; Morris *et al.*, 2004; Tumbar *et al.*, 2004). Bulge stem cells can contribute to cutaneous keratoacanthomas (Zito *et al.*, 2014) and can also act as cells of origin in squamous cell carcinomas (SCCs; Lapouge *et al.*, 2011; White *et al.*, 2011; Li *et al.*, 2013) during their activated state in a Pten-dependent manner (White *et al.*, 2014). However, additional mechanisms that control the ability of stem cells to contribute to skin tumors are poorly understood.

We and others have shown that the transcription factor Nfatc1 is expressed within bulge stem cells in mice and that Nfatc1 and its upstream phosphatase calcineurin regulate bulge stem cell activity during native hair cycling (Horsley *et al.*, 2008), aging

This article was published online ahead of print in MBoC in Press (http://www.molbiolcell.org/cgi/doi/10.1091/mbc.E15-05-0282) on August 26, 2015.

Conflict of interest: V.H. is a consultant for Unilever.

Address correspondence to: Valerie Horsley (valerie.horsley@yale.edu),

Abbreviations used: BrdU, 5-bromo-2′-deoxyuridine; cKO, conditional knockout; DETC, dendritic epidermal T-cell; DMBA, 7,12-dimethylbenz[a]anthracene; FACS, fluorescence-activated cell sorting; iKO, inducible knockout; MHC, major histocompatibility complex; mTmG, membrane Tomato/membrane enhanced green fluorescent protein; SCC, squamous cell carcinoma; Tcr, T-cell receptor; TPA, 12-*O*-tetradecanoylphorbol 13-acetate.

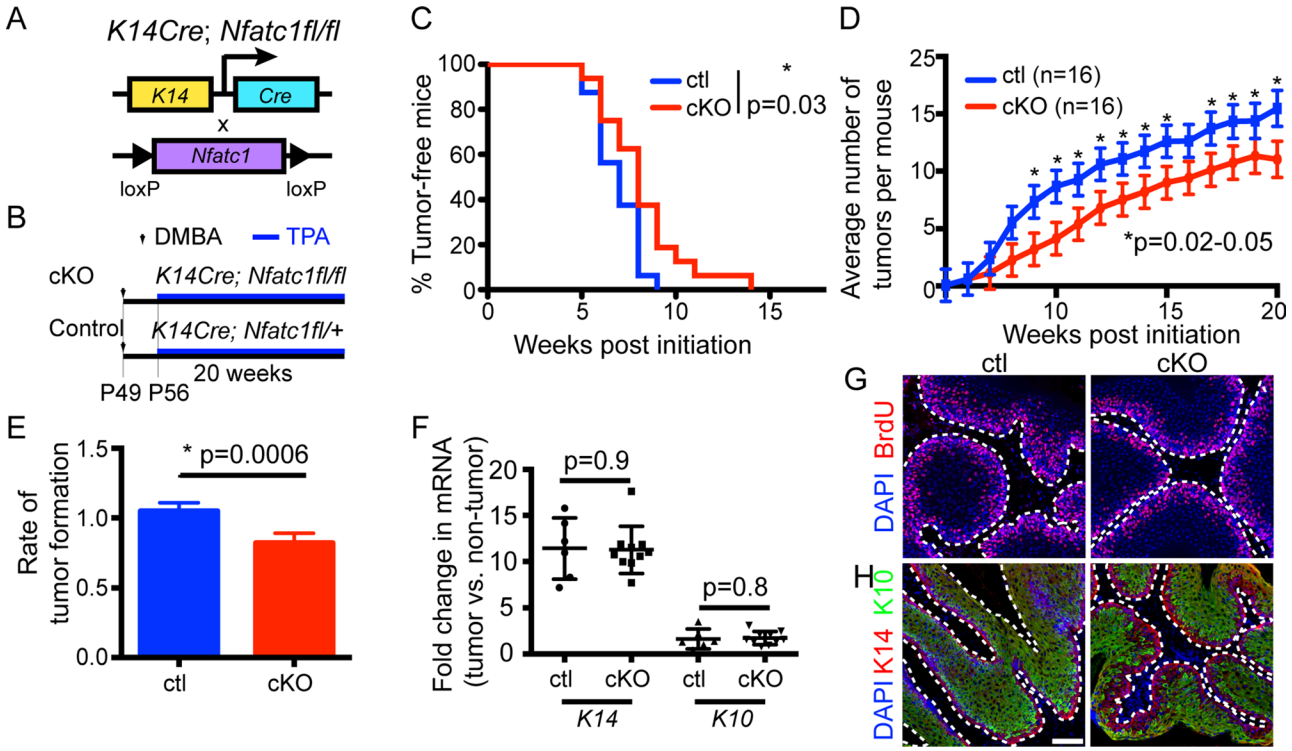

FIGURE 1: Epidermal *Nfatc1* deletion decreases DMBA/TPA tumorigenesis. (A) Schematic of *K14*-specific *Nfatc1* deletion. (B) DMBA/TPA tumorigenesis regime. (C) Percentage of tumor-free cKO/control mice during DMBA/TPA tumorigenesis (16 mice/genotype). *$p = 0.03$; log-rank test. (D) Average tumor number in cKO/control mice. Data: mean ± SEM. The profiles ($p = 0.03$) and several time points were significantly different (*); mixed-effect model. (E) Tumor formation rate between cKO/control mice is significantly different, $p = 0.0006$; mixed-effect model; time: continuous variable. (F) Real-time PCR for *K14* and *K10* in cKO/control tumors. Data: mean ± SEM (3 mice/genotype). (G, H) Immunostaining for (G) BrdU (red) and (H) K14 (red) and K10 (green) in cross sections of cKO/control tumors 8–10 wk post-DMBA. DAPI, blue. Scale bar, 50 µm.

(Keyes *et al.*, 2013), and pregnancy (Goldstein *et al.*, 2014). Of interest, patients receiving immunosuppressive treatment with calcineurin inhibitors, such as cyclosporine A and FK506, experience a significantly elevated risk of developing SCCs over the normal population (Euvrard *et al.*, 2003).

Chemical carcinogenesis studies using 7,12-dimethylbenz[a] anthracene (DMBA), a tumor initiator that induces oncogenic *Hras* mutations, and 12-*O*-tetradecanoylphorbol 13-acetate (TPA), a phorbol ester that promotes cell proliferation (Abel *et al.*, 2009), have enabled researchers to further characterize the role of calcineurin signaling in epidermal tumorigenesis. Mice lacking *calcineurin B* in the skin epithelium developed more tumors than controls when treated with DMBA/TPA, and Nfat proteins were implicated in the repression of tumor formation (Wu *et al.*, 2010). However, mice overexpressing a constitutively active Nfatc1 isoform driven by the *Hoxb7* promoter in the skin epithelium developed spontaneous skin SCCs (Tripathi *et al.*, 2013). Thus it is unclear whether endogenous Nfatc1 in bulge stem cells inhibits or enhances skin tumorigenesis. To clarify the role of Nfatc1 in skin tumor formation, we subjected mice lacking *Nfatc1* in the epidermis (*Keratin14*-Cre; *Nfatc1*$^{fl/fl}$: *Nfatc1*, conditional knockout [cKO]; Figure 1A; Horsley *et al.*, 2008) to chemical carcinogenesis with DMBA/TPA (Abel *et al.*, 2009). Our comprehensive study suggests that Nfatc1 increases skin tumor initiation by regulating DMBA metabolism and enhancing stem cell contribution to tumorigenesis.

RESULTS

Reduced skin papilloma formation in the absence of epidermal *Nfatc1*

To determine whether endogenous expression of *Nfatc1* influences skin tumor susceptibility, we examined the response of *Nfatc1* cKO mice and heterozygous littermates to DMBA/TPA carcinogenesis (Figure 1B). Treating 7-wk-old mice in the telogen stage of the hair cycle with a single dose of DMBA followed by a biweekly dose of TPA for 20 wk (Abel *et al.*, 2009) resulted in papilloma formation in control mice after 6 wk (Figure 1C). However, the majority of *Nfatc1* cKO mice treated with DMBA/TPA developed tumors after 8–10 wk (Figure 1C). Analysis of the number of tumors in control and *Nfatc1* cKO mice during a 20-wk time course using mixed-effect models revealed that *Nfatc1* cKO mice developed fewer tumors at multiple time points after week 8 and that the profiles for tumor formation between the control and cKO mice were significantly different (Figure 1D).

Because tumor formation increased for both control and *Nfatc1* cKO mice over time, we used a mixed-effect model with higher statistical power by maintaining time as a continuous variable to determine whether the rate of tumor formation or tumor number per week was altered in *Nfatc1* cKO mice. After week 5, *Nfatc1* cKO mice developed 20% fewer tumors per week than control mice (Figure 1E). Thus the rate of tumor formation was significantly reduced in *Nfatc1* cKO mice compared with control mice. Characterization of papillomas from control and *Nfatc1* cKO mice 8–10 wk

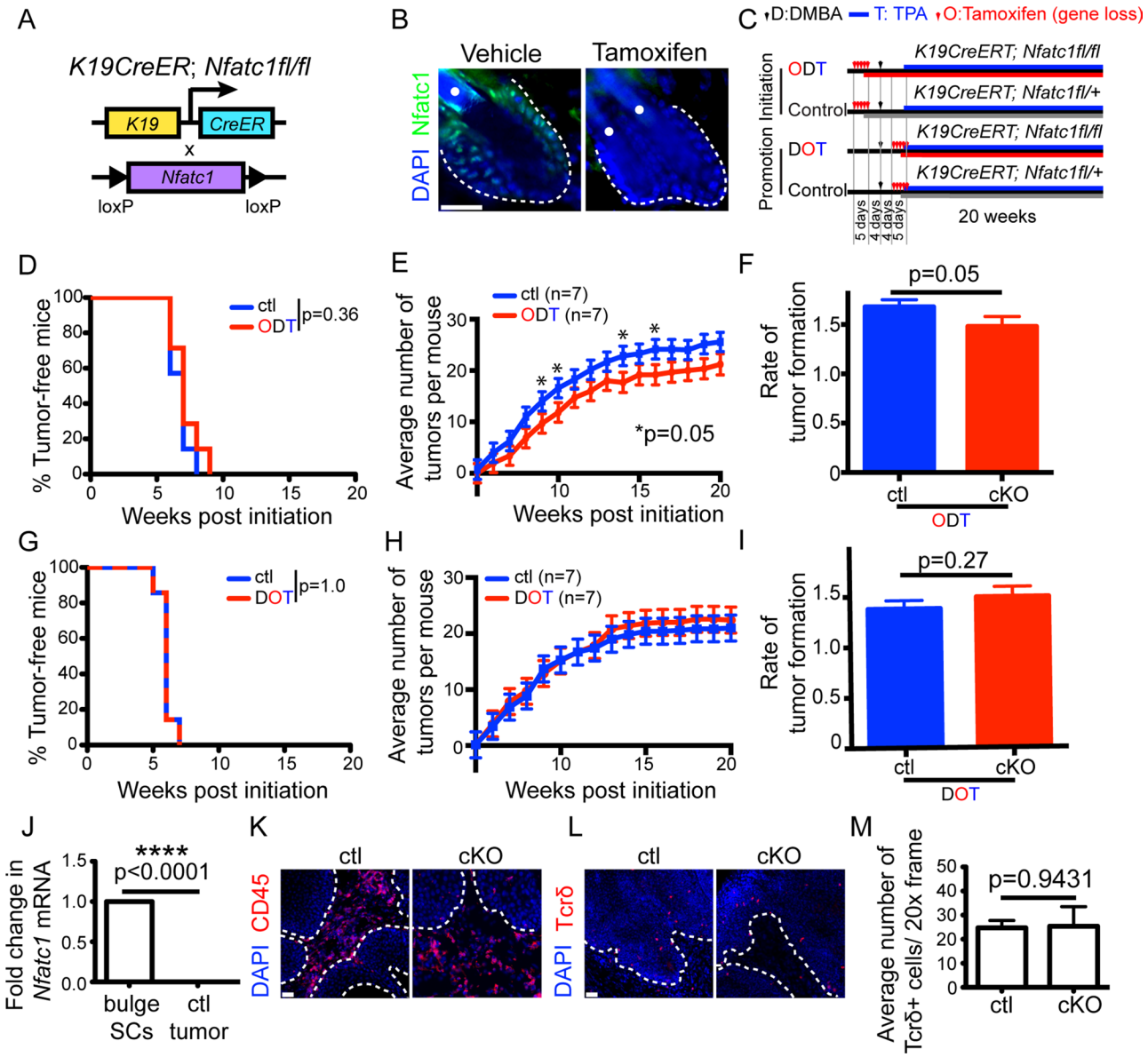

FIGURE 2: *Nfatc1* deletion decreases the rate of tumor initiation but not tumor promotion. (A) Schematic of inducible *K19*-specific *Nfatc1* deletion. (B) Nfatc1 immunostaining (green) in iKO mice 5 d after tamoxifen/vehicle. (C) DMBA/TPA initiation (ODT) and promotion (DOT) regimes. (D, G) Percentage of tumor-free iKO/control mice in (D) ODT or (G) DOT regime ($n = 16$ mice/genotype). (E, H) Average tumor number during (E) ODT or (H) DOT regime. Data: mean ± SEM (seven mice/genotype). Several time points were significantly different (*); mixed-effect model. (F, I) Tumor formation rate during (F) ODT regime is significantly different but not during (I) DOT regime (mixed-effect model; time: continuous variable). (J) Real-time PCR of *Nfatc1* in tumor cells relative to FACS-sorted bulge cells. Data: mean ± SD (six mice/group). Immunostaining for (K) CD45 (red) and (L) Tcrδ (red) in cKO/control tumors 8–10 wk post-DMBA. (M) Quantification of Tcrδ+ cells in cKO/control tumors. Data: mean ± SEM (three mice/genotype). DAPI, blue; dotted line, epithelial–stromal barrier; white dots, hair shaft autofluorescence. Scale bar, 25 μm (B), 50 μm (K, L).

after DMBA treatment indicated similarities in tumor size (unpublished data), proliferation (Figure 1G), and *K14* and *K10* mRNA and protein expression (Figure 1, F and H).

Nfatc1 enhances the rate of skin tumor initiation but not promotion

To determine whether Nfatc1 affects skin tumorigenesis before or after DMBA initiation (Zoumpourlis *et al.*, 2003), we crossed *K19*CreERT mice (Means *et al.*, 2008) with *Nfatc1*$^{fl/fl}$ mice to generate *Nfatc1* inducible knockout (*Nfatc1* iKO mice; Figure 2A). We confirmed that tamoxifen treatment reduced Nfatc1 expression within hair follicle bulge cells in *Nfatc1* iKO mice relative to vehicle-treated controls (Figure 2B). To test whether Nfatc1 regulates tumor initiation, we treated *Nfatc1* iKO mice with tamoxifen to induce Cre recombinase activity and subsequent *Nfatc1* deletion before DMBA treatment (ODT; Figure 2C). In contrast, to determine whether Nfatc1 controls tumor promotion, we treated *Nfatc1* iKO mice with tamoxifen after DMBA treatment (DOT; Figure 2C).

When *Nfatc1* was deleted before DMBA treatment (ODT; Figure 2C), *Nfatc1* iKO mice and control mice developed tumors

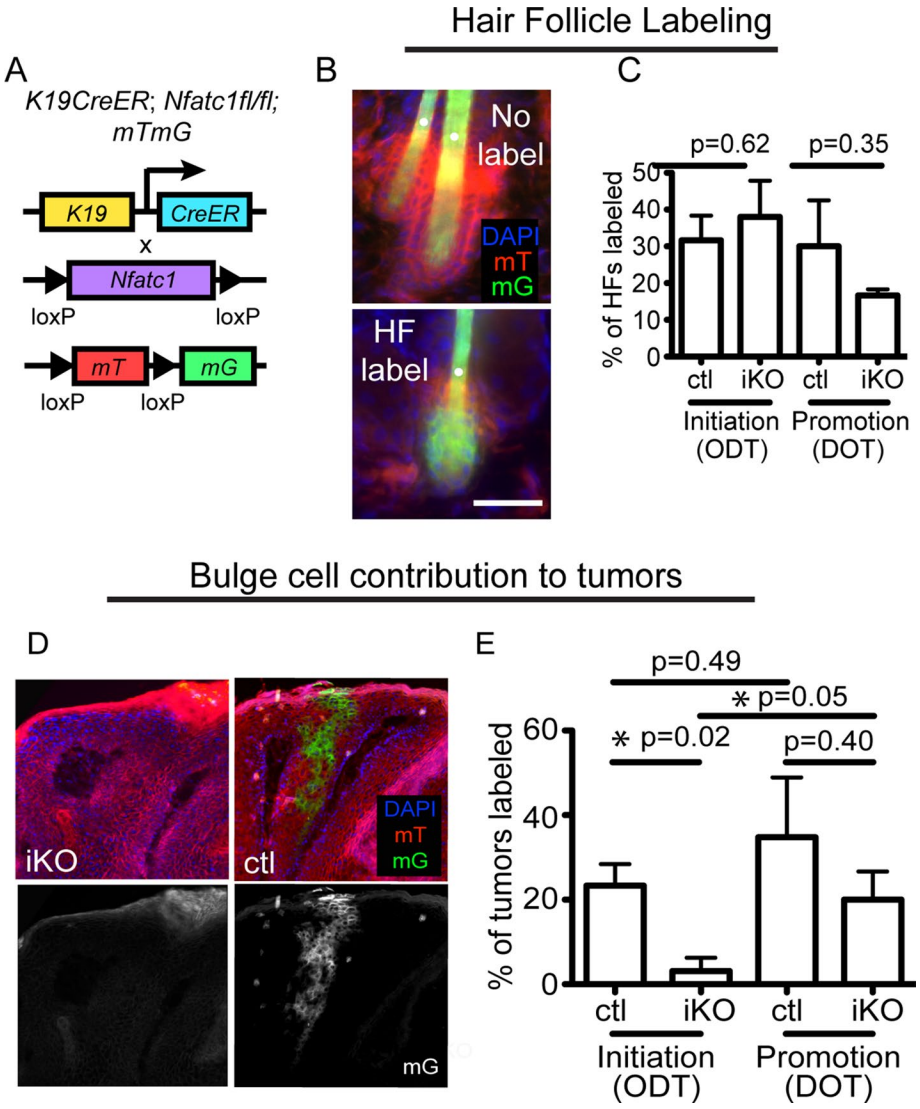

FIGURE 3: *Nfatc1* deletion decreases stem cell contribution to papillomas during tumor initiation. (A) Schematic of inducible *K19*-specific *Nfatc1* deletion and *mTmG* labeling. (B) Representative images of *K19*CreERT;*mTmG* follicles after tamoxifen. Images show unlabeled (only mT+ cells) or labeled (containing mG+ cells) follicles. (C) Percentage of mG+ hair follicles 8–12 wk post-DMBA (initiation, ODT; promotion, DOT). Data are mean ± SEM for 50–100 hair follicles from four individual mice/group. (D) Representative sagittal section of a tumor containing mG+ cells derived from *K19*-expressing bulge cells. (E) Percentage of tumors containing mG+ cells in iKO mice and littermate controls from sagittally sectioned tumors during ODT and DOT regimes. Data are mean ± SEM of three or four individual mice/genotype for 8–15 tumors from each mouse. Tumors were harvested 8–12 wk post-DMBA. DAPI, blue. White dots denote hair shaft autofluorescence. Scale bar, 25 μm.

between 6 and 8 wk (Figure 2D). However, *Nfatc1* iKO mice developed fewer papillomas than littermate controls at several time points during TPA treatment (Figure 2E). In addition, the rate of tumor formation was significantly reduced in *Nfatc1* iKO mice when *Nfatc1* was deleted before DMBA treatment (Figure 2F). Reduced Cre activity in the inducible *K19*CreERT mouse model may explain why the reduction in skin tumorigenesis is not as significantly reduced as with the *K14*Cre model. However, when *Nfatc1* was deleted after DMBA treatment but before TPA treatment (DOT; Figure 2C), *Nfatc1* iKO mice developed a similar number of papillomas at the same rate as littermate control mice (Figure 2, G–I). Collectively these data suggest that Nfatc1 regulates the rate of tumor initiation and does not affect tumor promotion.

Consistent with the inability of Nfatc1 to affect tumor promotion, *Nfatc1* mRNA was not detected within papillomas of control mice as compared with its high enrichment in bulge stem cells isolated by fluorescence activated cell sorting (FACS; Figure 2J). These results are similar to previous studies demonstrating that *Nfatc1* mRNA and protein levels are highly down-regulated in skin cancer stem cells relative to hair follicle stem cells (Schober and Fuchs, 2011). Because immune cells have been implicated as regulators of skin tumor formation (de Visser *et al.*, 2006; Ostrand-Rosenberg, 2008; Demehri *et al.*, 2009; Zamarron and Chen, 2011), we investigated whether epidermal deletion of *Nfatc1* modulated the presence of immune cells in skin tumors. Immunofluorescence staining for the pan–immune cell marker CD45 revealed the presence of hematopoietic cells in tumors from both *Nfatc1* cKO and control mice (Figure 2K). We also examined the presence of dendritic epidermal T-cells (DETCs), a subpopulation of T-cells that resides within the skin and expresses the γδ T-cell receptor (Tcr; Stingl *et al.*, 1987). Immunofluorescence staining and quantification of Tcrδ+ cells in papillomas from *Nfatc1* cKO mice and littermate controls revealed similar numbers of DETCs within the tumor (Figure 2, L and M). These data suggest that *Nfatc1* regulates tumor formation at the earliest stages of development rather than by affecting tumor promotion via alterations in the tumor immune cell stroma.

Nfatc1 enhances bulge cell contribution to tumors in vivo

We next analyzed whether Nfatc1 could regulate follicular stem cell contribution to tumors. To this end, we used a genetic lineage tracing approach to trace bulge stem cells and their progeny during tumorigenesis in control and *Nfatc1* iKO mice. Specifically, we crossed *Nfatc1* iKO mice to mice ubiquitously expressing a fluorescent membrane Tomato/membrane enhanced green fluorescent protein GFP (GFP; *mTmG*) reporter construct (Muzumdar *et al.*, 2007; Figure 3A). In the absence of Cre activity, all cells express mT. However, treatment with tamoxifen induces *K19*CreERT activity, resulting in a heritable loss of *mT* expression and the induction of *mG* expression in *K19*-expressing bulge stem cells and their progeny. These mice were subjected to both the initiation and promotion tumorigenesis regimes (Figure 2C). After tamoxifen treatment, a similar percentage of hair follicles in both genotypes contained mG+ cells (Figure 3, B and C). Furthermore, we observed the contribution of *K19*-expressing bulge cells to skin tumors after 8–12 wk of the carcinogenesis regime (Figure 3D), and quantification of skin tumor labeling revealed a decrease in bulge

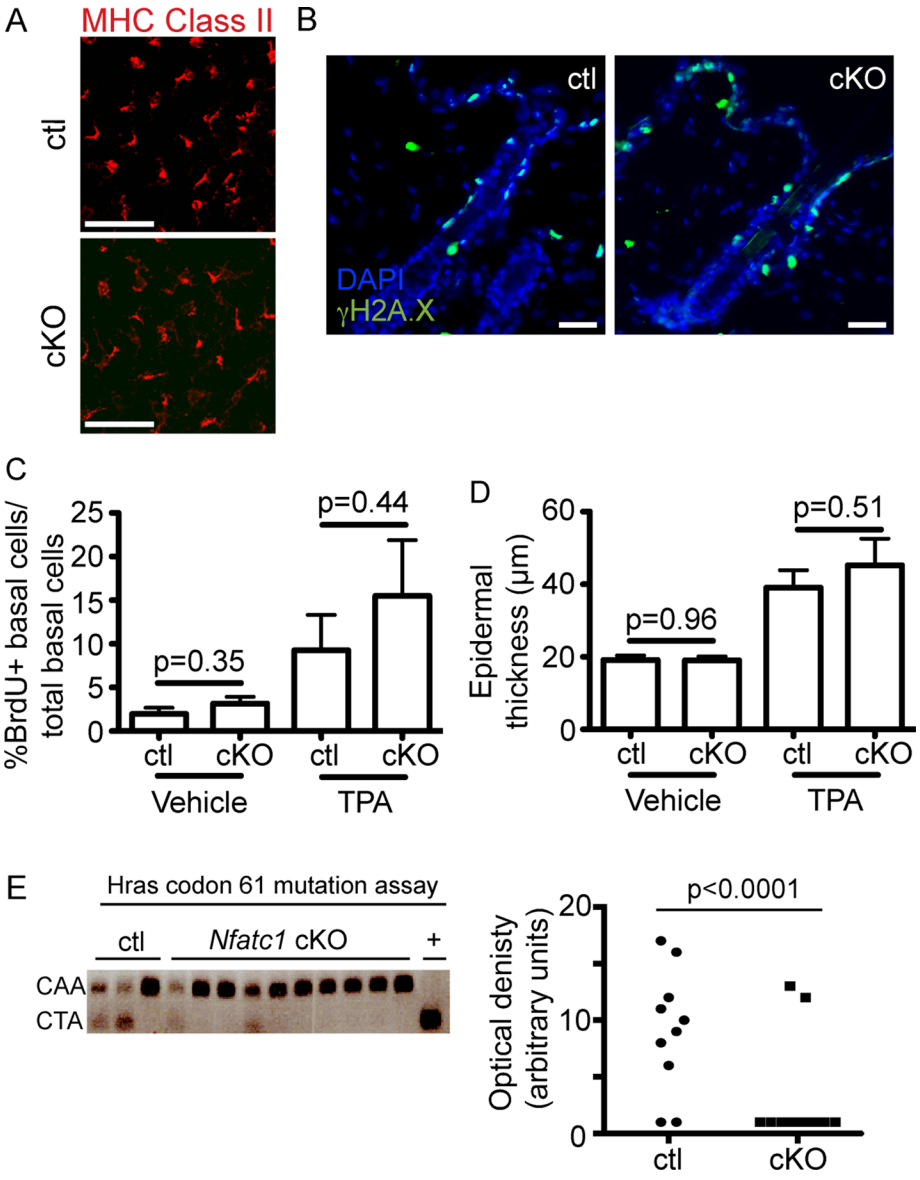

FIGURE 4: Epidermal *Nfatc1* deletion reduces DMBA-induced *Hras* codon mutations. (A) MHC class II immunostaining (red) from cKO/control epidermal sheets. (B) γH2A.X immunostaining (green) in cKO/control mice 24 h post-DMBA/vehicle. (C) Percentage of BrdU+ epidermal cells normalized to total basal cells 24 post-TPA/vehicle. Data: mean ± SEM (three or four mice/group; >4000 cells quantified/ mouse). (D) Epidermal thickness 24 h post-TPA/vehicle. Data: mean ± SEM (four mice/group). (E) *Hras* codon 61 mutations from cKO/control tumors 8–10 wk post-DMBA. +, CarC DNA. Optical density of CTA mutant bands. Chi-squared test. DAPI, blue. Scale bar, 50 μm.

cell contribution to tumors in *Nfatc1* iKO mice during the initiation regime (Figure 3E). However, *Nfatc1* deletion after tumor initiation (DOT) did not affect bulge stem cell contribution to tumors (Figure 3E). Together these findings indicate that *Nfatc1* expression in hair follicle stem cells enhances their ability to contribute to skin papillomas during tumor initiation.

Loss of *Nfatc1* alters *Hras* codon mutations in response to DMBA

The initiating events for mouse skin tumors induced by DMBA largely involve mutation of the *Hras* gene at codon 61 (Balmain *et al.*, 1984). These mutations are caused by metabolites generated by cytochrome P-450 enzymes such as Cyp1a1 and Cyp1b1 and microsomal epoxide hydrolase (Epxh1) after engagement of the aryl hydrocarbon receptor (Ahr) and the aryl hydrocarbon receptor nuclear translocator (Arnt) within keratinocytes and epidermal Langerhans cells (Modi *et al.*, 2012).

To determine whether the reduced rate of tumor initiation in *Nfatc1* cKO mice results from alterations in DMBA metabolism, we analyzed Langerhans cells, which metabolize DMBA and enhance chemical carcinogenesis (Modi *et al.*, 2012). To this end, we immunostained epidermal sheets from *Nfatc1* cKO mice (Figure 1A) with antibodies against major histocompatibility complex (MHC) class II, which marks Langerhans cells within the skin epithelium. No changes in the presence of MHC class II+ Langerhans cells were observed between *Nfatc1* cKO and control mice (Figure 4A).

DNA damage occurs in keratinocytes after DMBA treatment (Hennings *et al.*, 1993). To analyze the response of keratinocytes to DMBA in *Nfatc1* cKO mice (Figure 1A), we treated mice with a single topical dose of carcinogen and analyzed DNA damage after 24 h by immunostaining for γH2A.X, a histone variant induced by DNA damage. No global differences in the presence of γH2A.X+ cells were observed between control and *Nfatc1* cKO mice after either vehicle or DMBA treatment (Figure 4B). To determine whether a difference in TPA responsiveness could account for the decreased tumor formation observed in *Nfatc1* cKO mice, we pulsed mice with 5-bromo-2′-deoxyuridine (BrdU) to mark proliferating cells after one application of TPA or a vehicle control. Quantification of BrdU+ cells in the epidermis revealed equivalent levels of proliferation between *Nfatc1* cKO mice and littermate controls 24 h after either vehicle or TPA treatment (Figure 4C). Similarly, no significant differences in epidermal thickness were observed between *Nfatc1* cKO mice and littermate controls under vehicle or TPA-treated conditions (Figure 4D).

To further examine the response of *Nfatc1* cKO mice to DMBA-induced tumorigenesis, we analyzed tumors from control and *Nfatc1* cKO mice for the presence of DMBA-induced mutations in *Hras* codon 61 from CAA to CTA, which creates a new *Xba*1 restriction enzyme site (Sachs *et al.*, 2012). Whereas the mutant *Hras* codon was detected in a majority of tumors in control mice, few tumors from *Nfatc1* cKO mice displayed detectable *Hras* mutations (Figure 4E). These data indicate that DMBA-induced skin tumors from *Nfatc1* cKO mice exhibit fewer *Hras* codon 61 mutations than littermate controls.

Nfatc1 regulates expression of DMBA-metabolizing enzymes

Because DMBA metabolism is responsible for the induction of mutations in *Hras* during chemically induced tumorigenesis, we next

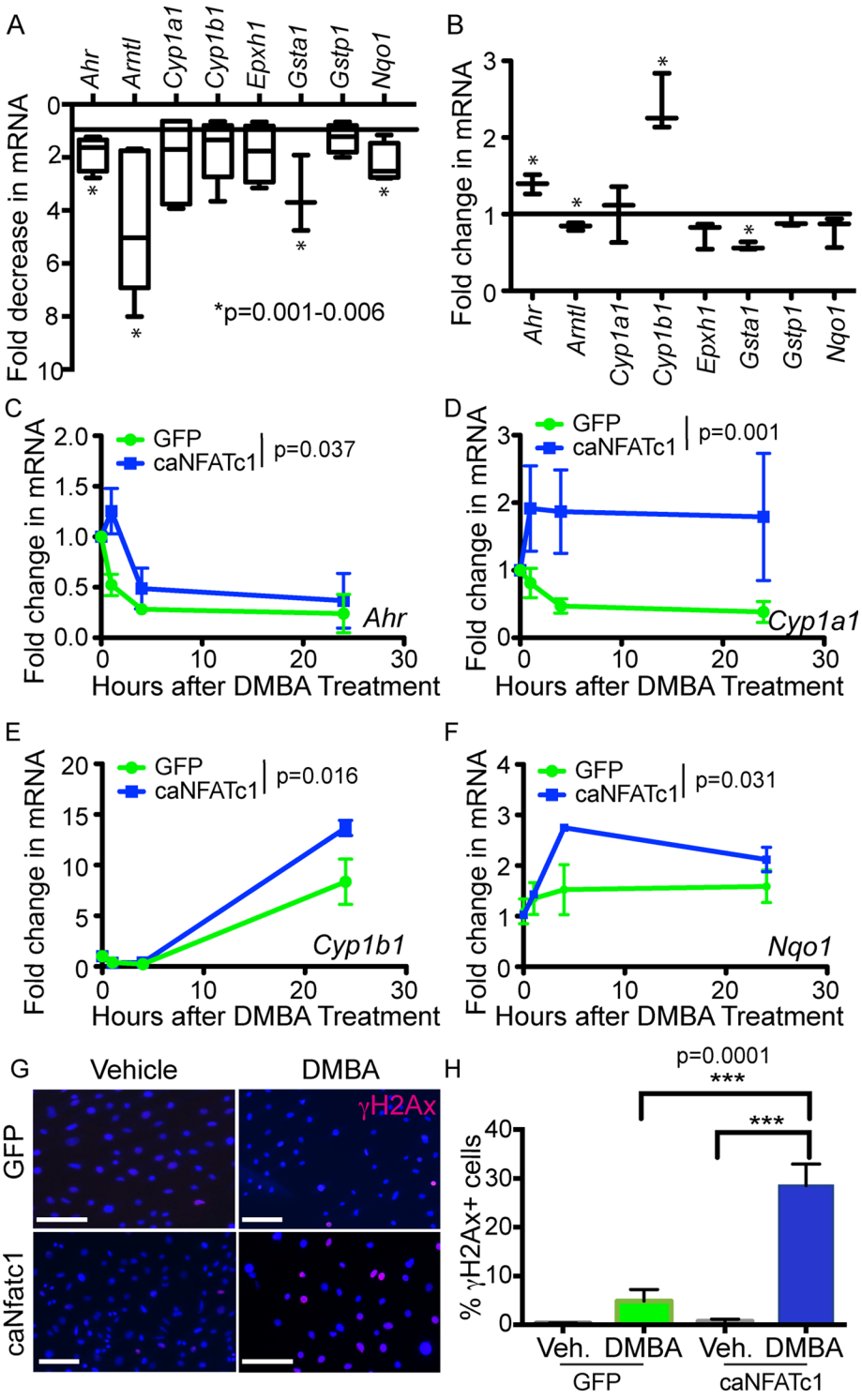

FIGURE 5: Nfatc1 regulates expression of DMBA-metabolizing enzymes. (A) Real-time PCR analysis of mRNA expression for DMBA-metabolizing enzymes in FACS-purified sorted cKO bulge cells compared with control bulge cells. Data are mean ± SD (three or four mice/genotype). *$p < 0.05$; one-way ANOVA. (B) Real-time PCR for DMBA-metabolizing enzymes in caNFATc1 compared with control-infected keratinocytes. *$p < 0.05$; one-way ANOVA. (C–F) Real-time PCR for (C) *Ahr*, (D) *Cyp1a1*, (E) *Cyp1b1*, and (F) *Nqo1* mRNA in caNFATc1- and control-infected keratinocytes at 0, 1, 4, and 24 h. The *p* value reflects two-way ANOVA for the effect of Nfatc1 expression. (G) γH2A.X immunostaining (red) in GFP- and caNFATc1-infected keratinocytes 24 h post-DMBA/vehicle. DAPI, blue. Scale bar, 50 μm. (H) Quantification of γH2A.X+ GFP- and caNFATc1-infected keratinocytes after 24 h in vehicle or DMBA. Data: mean ± SEM (three or four replicates for each treatment in two independent experiments; >179–1435 cells analyzed). One-way ANOVA.

analyzed expression of genes involved in DMBA metabolism by real-time PCR. We found that expression of *Ahr*, *Arntl*, *Gsta1*, and *Nqo1* is significantly down-regulated in bulge cells from *Nfatc1* cKO mice relative to littermate controls (Figure 5A). To probe whether Nfatc1 could drive expression of these DMBA-metabolizing enzymes, we infected mouse keratinocytes with retrovirus expressing either a constitutively active form of NFATc1 (caNFATc1; Horsley *et al.*, 2008) or an empty vector GFP control (Figure 5B). From these analyses, we observed a significant increase in *Ahr* and *Cyp1b1* expression and a decrease in *Arntl* and *Gsta1* expression (Figure 5B). We next investigated whether caNFATc1 influenced expression of these DMBA-metabolizing enzymes 1, 4, and 24 h after DMBA treatment. Four of these genes (*Ahr*, *Cyp1a1*, *Cyp1b1*, and *Nqo1)* were significantly more highly expressed in caNFATc1-expressing keratinocytes after DMBA treatment relative to controls. caNFATc1 expression also increased the percentage of DMBA-treated keratinocytes with γH2Ax nuclear foci, indicating that Nfatc1 expression promotes DNA damage after DMBA treatment (Figure 5, G and H). Taken together, these data suggest that Nfatc1 controls the expression of genes involved in DMBA metabolism, leading to enhanced DNA damage after DMBA exposure.

DISCUSSION

Here we identify a role for Nfatc1 during the initiation of chemically induced epidermal tumorigenesis. The tumor-enhancing roles for Nfatc1 in the skin are distinct from the role of calcineurin, the upstream phosphatase that regulates Nfat's nuclear localization, which inhibits skin tumorigenesis (Wu *et al.*, 2010). Patients treated with calcineurin inhibitors have an increased disposition for developing SCCs (Euvrard *et al.*, 2003), and mouse and human cell studies have revealed that genetic and pharmacological inhibition of calcineurin/Nfat signaling increases chemically induced skin tumor onset (Wu *et al.*, 2010). Using the same chemical tumorigenesis paradigm as Wu *et al.* (2010), we find that mice lacking *Nfatc1* in the epidermis do not display enhanced tumor formation but instead have reduced tumor formation, suggesting that calcineurin may inhibit skin tumorigenesis through its regulation of additional Nfat isoforms or other proteins, such as Atf3 or p53.

Our data and those of others (Li *et al.*, 2013) are consistent with cells from the bulge and outside the bulge contributing to

DMBA-induced tumors. Several types of keratinocytes are likely origins of SCCs, including those outside of the bulge (Lapouge *et al.*, 2011; White *et al.*, 2011). Although inefficient Cre activity could yield heterogeneity in our lineage tracing data, loss of *Nfatc1* before tumor initiation decreases the contribution of bulge stem cells and their progeny to skin tumors. The minor fraction of keratinocytes that express Nfatc1 in the bulge and contribute to tumors in this model may explain the moderate reduction in tumorigenesis in *Nfatc1* cKO mice.

Recent data reveal that follicular stem cell activation is required for stem cell–induced tumor initiation (White *et al.*, 2014). Nfatc1 is a major driver of follicular stem cell quiescence (Horsley *et al.*, 2008; Keyes *et al.*, 2013), and the reduced rate of tumorigenesis after *Nfatc1* deletion seems contrary to its role in stem cell activity. Because we treated both *Nfatc1* cKO mice and littermate controls with DMBA during telogen and promoted tumorigenesis with TPA, which enhances proliferation throughout the skin epithelium (Figure 4C) and induces hair follicle stem cell activity (Stenn and Paus, 2001), our study did not elucidate whether Nfatc1's role in stem cell activation influences tumor formation. White *et al.* (2014) used an inducible genetic mouse model to express an oncogenic *Kras* allele in hair follicle stem cells to dissect the requirement of stem cell activity during skin tumorigenesis. Whether Nfatc1 alters SCC formation in other tumor induction paradigms, including a genetically activated *Ras* mouse model, will be an interesting area of future study.

Our findings are consistent with previous work demonstrating that Nfatc1 enhances tumorigenesis in multiple cell types (Mancini and Toker, 2009; Muller and Rao, 2010). In fibroblasts, constitutive Nfatc1 activation induces cellular transformation through disruption of contact-mediated cell growth (Neal and Clipstone, 2003). Nfatc1 can also promote cancer cell invasion in breast and lung cancer cell lines (Oikawa *et al.*, 2013) and promote angiogenesis in tumor-associated vasculature (Ryeom *et al.*, 2008). Furthermore, Nfat activation has been associated with lymphomas (Marafioti *et al.*, 2005; Pham *et al.*, 2005), leukemias (Medyouf *et al.*, 2007), and pancreatic cancers (Buchholz *et al.*, 2006; Koenig *et al.*, 2010).

Our data also resonate with a recent study demonstrating that constitutive overexpression of a nuclear form of Nfatc1 is sufficient to drive the formation of SCC-like tumors in the skin (Tripathi *et al.*, 2013). Although Nfatc1 was implicated in the creation of a proinflammatory microenvironment in the skin through regulation of cytokine gene expression (Tripathi *et al.*, 2013), our studies suggest that endogenous Nfatc1 promotes bulge cell contribution to tumors in a role independent of inflammation. We do not detect overt alterations in skin inflammatory response (Horsley *et al.*, 2008) or cytokine gene expression during homeostasis after Nfatc1 inhibition (Goldstein *et al.*, 2014) or inflammation during tumorigenesis in *Nfatc1* cKO mice.

In our study, we discovered a link between Nfatc1 and DMBA-induced DNA damage within follicular stem cells. Polyaromatic hydrocarbons such as DMBA are highly prevalent in industrial pollution and are detoxified into adducts that cause DNA damage by several enzymes that are induced in part by the transcription factor Ahr. Indeed, mice treated with extracts of airborne particles from industrial pollution form SCCs in an *Ahr*-dependent manner (Matsumoto *et al.*, 2007). We show that Nfatc1 enhances the expression of *Ahr* and its downstream target *Cyp1a* in DMBA-treated keratinocytes and leads to an elevated DNA damage response in DMBA-treated keratinocytes. The role of Nfatc1 in regulating DNA damage is likely balanced by additional mechanisms in bulge cells to promote DNA repair, such as elevated expression of Bcl-2 (Sotiropoulou *et al.*, 2010) and stabilization of p53 (Petersson *et al.*, 2015). Of interest, Nfatc1 can directly regulate the expression of the cytochrome P450 superfamily member CYP2E1 (Wang *et al.*, 2010), which metabolizes ethanol and other small polar molecules, suggesting that Nfatc1 may be involved broadly in metabolism of xenobiotics. Defining whether Nfatc1 directly or indirectly regulates the expression of P450 family members to affect skin tumorigenesis may reveal novel mechanisms involved in skin tumor initiation.

MATERIALS AND METHODS

Animal use

All animals were housed and handled according to the institutional guidelines of Yale University. *Nfatc1*$^{fl/fl}$ (Aliprantis *et al.*, 2008), *Keratin14*Cre (Vasioukhin *et al.*, 1999), *Keratin19*CreERT (Means *et al.*, 2008), and *mTmG* (Muzumdar *et al.*, 2007) mice have been described previously. For *K14*Cre/*Nfatc1* and *K19*CreERT/*Nfatc1* tumorigenesis studies, mice were maintained in the outbred CD-1 background, and age- and sex-matched Cre+; *Nfatc1*$^{fl/+}$ littermates were used as controls. For the *K19cre*ERT/Nfatc1/mTmG lineage tracing experiments, mice were in a mixed CD-1, 129×1/SvJ background. Activation of CreERT was performed by topical administration of tamoxifen (10 mg/ml in ethanol; Sigma-Aldrich, St. Louis, MO) for 5 d. For BrdU experiments, mice were injected intraperitoneally with 50 mg/kg BrdU (Sigma-Aldrich) for 4 h before being killed.

Chemical carcinogenesis

To induce skin tumors, both control and *Nfatc1* cKO mice in the telogen phase of the hair cycle (Horsley *et al.* 2008) were shaved on the back and administered one topical dose of DMBA (20 µg in 100 µl acetone; Sigma-Aldrich). Mice received topical treatments of TPA (5 µg in 100 µl ethanol; Sigma-Aldrich) twice weekly for 20 wk, and tumors were counted weekly. Histological analyses of tumors from *Nfatc1* cKO and control mice were performed by a veterinary pathologist and revealed the presence of skin papillomas. One control mouse developed an SCC, which metastasized to the lung and inguinal lymph nodes.

Histology and immunofluorescence

For epidermal thickness analyses and immunofluorescence, tissues were embedded in OCT compound (Tissue-Tek; Sakura Finetek, Torrance, CA), frozen, sectioned, fixed in 3.7% formaldehyde, and stained with hematoxylin and eosin. When applicable, the M.O.M. kit (Vector Labs, Burlingame, CA) was used to prevent nonspecific binding of mouse secondary antibodies. The following primary antibodies were used: BrdU (rat, Bu 1/75 [ICR1], 1:300; Abcam, Cambridge, MA); CD45 (rabbit, 30-F11, 1:250; eBioscience, San Diego, CA); γδTcr (hamster, GL3, 1:200; BD Biosciences, San Jose, CA); γH2A.X (mouse, JBW301, 1:100; Millipore, Billerica, MA); keratin 14 (chicken, 1:500; kind gift of Julie Segre, National Institutes of Health); keratin 10 (rabbit, 1:500; kind gift of Julie Segre), and Nfatc1 (mouse, 7A6, 1:25; Santa Cruz Biotechnology, Santa Cruz, CA). For BrdU staining, tissue sections were incubated in 2 N HCl (37°C, 30 min) and 0.1 M sodium borate, pH 8.5 (room temperature, 10 min), before primary antibody incubation. The following secondary antibodies were used: anti-chicken, anti-rabbit, anti-mouse, anti-rat, and anti-hamster conjugated to rhodamine red X or Alexa 488 (1:250; Jackson ImmunoResearch, West Grove, PA). Sections were mounted in Prolong Gold anti-fade reagent with 4′,6′-diamidino-2-phenylindole (DAPI; Life Technologies, Grand Island, NY). Imaging was performed on a Zeiss Imager M.1 fluorescence microscope (Zeiss, Oberkochen, Germany), and images were acquired with an AxioCam MR3 camera and quantified with ImageJ (National Institutes of Health, Bethesda, MD).

Quantification of Langerhans cells in epidermal sheets

Mouse ears were collected, split into dorsal and ventral sides, and floated epidermal side up on a Ca^{2+}/Mg^{2+}-free phosphate-buffered saline (PBS) solution containing 20 mM EDTA for 2 h at 37°C. Epidermal sheets were gently peeled from the dermis, washed in PBS containing Ca^{2+}/Mg^{2+}, and fixed in cold acetone for 20 min at –20°C. Sheets were washed in PBS, incubated for 1 h at 37°C in 2% (wt/vol) bovine serum albumin (BSA) in PBS, and stained overnight at 4°C with MHC class II (1-A/1-E) primary antibody (rat, M5/114.15.2, 1:200; eBioscience, San Diego, CA). After being washed in PBS, sheets were stained overnight at 4°C with a rhodamine red X–conjugated anti-Rat secondary antibody (1:250; Jackson ImmunoResearch) in 1% (wt/vol) BSA in PBS. After washing in PBS, epidermal sheets were mounted on slides with Prolong Gold anti-fade reagent (Life Technologies) and visualized by confocal microscopy.

Analysis of DMBA responsiveness in vivo and *Hras* codon mutations

To analyze the response of DMBA-metabolizing enzymes to DMBA treatment in control and *Nfatc1* iKO mice, we treated back skin with vehicle and DMBA and isolated mRNA after 24 h. Analysis of mutations in *Hras1* was performed as described previously (Sachs *et al.*, 2012). Briefly, genomic DNA was isolated from skin tumors 8–10 wk after DMBA treatment using phenol-chloroform-isoamyl alcohol (Life Technologies). Codon 61 of *Hras1* was amplified by nested PCR using *Hras* primer pairs 1 and 2 (Supplemental Table S1). Amplification with *Hras* primer pair 1 generated a 267–base pair product. Subsequent nested PCR amplification with *Hras* primer pair 2 generated a 178–base pair product. A 5-µg amount of DNA was digested at 37°C overnight with the restriction enzyme *Xba*1 and resolved on a 2% agarose gel. Genomic DNA from CarC cells (provided by M. Girardi, Yale University), which contains mutations at both *Hras* alleles, was used as a positive control.

FACS, RNA isolation, cDNA synthesis, and real-time PCR

For bulge stem cell isolation, subcutaneous fat was gently removed from skins with a scalpel. Skins were floated on 0.25% trypsin-EDTA overnight at 4°C and for 1 h at 37°C. Trypsin was inactivated with medium containing chelexed fetal bovine serum (FBS), and epidermal cells were gently removed from the skins with a scalpel. Cells were filtered and resuspended as single-cell suspensions in staining buffer (SB) containing PBS/4% chelexed FBS. Cells were incubated with the following antibodies for 30 min on ice in the dark: CD34-biotin (1:50; eBioscience) and Cd49f-PE (1:75; BD Biosciences). Cells were washed, resuspended in SB, and incubated with streptavidin-APC (1:200; BD Biosciences) for 30 min on ice in the dark. Cells were washed and resuspended at 1×10^6 cells/ml. Propidium iodide, 0.5 g/ml (Sigma-Aldrich), was added to the cell suspension immediately before sorting. Cells were sorted on a FACS Aria III equipped with FACS DiVA software (BD Biosciences).

For RNA isolation from FACS-sorted cells, 150,000 bulge cells were sorted into 600 µl of TRIzol LS (Life Technologies). For tumor RNA isolation, papillomas and nontumor skins from *Nfatc1* cKO mice and littermate controls were homogenized in TRIzol (Life Technologies). Total RNAs were extracted according to manufacturer's protocol and purified using the RNeasy kit (Qiagen, Venlo, Netherlands).

To generate cDNA, equal amounts of RNA were reverse transcribed using oligo(dT) primers (Superscript III First-Strand Synthesis Kit; Life Technologies). Real-time PCR was performed on a Light Cycler 480 II using SYBR GREEN reagents (Roche, Indianapolis, IN). Primers used are listed in Supplemental Table S1. Relative quantification was calculated with the $\Delta\Delta Ct$ method using β-actin as a reference gene.

Cell culture

MSCV-GFP (control) and constitutively active NFATc1 (caNFATc1) retroviral vectors have been described previously (Neal and Clipstone, 2003; Horsley *et al.*, 2008). Briefly, retroviral vectors were transfected with Xtremegene HD (Roche) into Phoenix cells to generate retroviral supernatants. Supernatants were filtered at 0.45 µm, and infections of primary mouse keratinocytes were performed by adding retroviral supernatant, chelexed FBS, and 4 µg/ml Polybrene and centrifuging at $800 \times g$ for 30 min at 32°C. After centrifugation, retroviral supernatant was removed, and keratinocytes were refed with growth medium. Cells were grown for 48 h before collection in TRIzol (Invitrogen) for RNA isolation. For in vitro DMBA treatments, MSCV-GFP– or caNFATc1–infected cells were treated with 0.15 µg/ml DMBA for indicated time points up to 24 h.

Statistical analysis

For tumor frequency, statistical analyses were performed using a log-rank test. Analysis of differences in *Hras* codon mutations between control and cKO mice was performed using the chi-square test. Statistical analyses between two groups were performed using a Student's *t* test, between multiple groups using a one-way analysis of variance (ANOVA), or between groups over time with a two-way ANOVA. To assess the differences in tumor number over time between control and cKO mice, we used a mixed-effect model with genotype and week as (discrete) fixed effects and a random intercept for each mouse. This model, conceptually similar to a repeated-measures ANOVA, allows us to estimate the tumor number difference at each week taking into account the within-mouse correlation and can account for missing values. In addition, the weekly rate of tumor formation after week 5 was evaluated using the equation $N_{it} = \alpha_o + \beta_1 t + \beta_2 t(G_{KO}) + u_i + \varepsilon_{it}$, where N_{it} is the number of tumors per week for mouse i, α_o is the intercept, u_i is a random term for each mouse, β_1 represents the rate for the control mice, t is the time after week 5, β_2 is the difference in tumor number per week between groups, $G_{KO} = 1$ for KO mice and 0 for control mice, and ε_{it} is the error term. The mixed-model approach using R and all other analyses were performed using GraphPad Prism version for Macintosh (GraphPad, La Jolla, CA). For all analyses, $p \leq 0.05$ was accepted for statistical significance.

ACKNOWLEDGMENTS

We thank Z. Zhou and K. Nelson (Yale Cell Sorting Facility) for FACS sorting and G. Rivera, A. Graham, and A. Chun for technical assistance. M. Girardi graciously provided DNA from CarC cells. Horsley lab members provided valuable discussions and critical reading of the manuscript. R.Z. is funded by the Lo Graduate Fellowship in Excellence in Stem Cell Research. J.G. was funded by National Institutes of Health Training Grant 5T32HG 3198-7. V.H. was a Pew Scholar in Biomedical Research and is funded by the National Institutes of Health (AR060295) and the Connecticut Department of Public Health (12SCBYALE01).

REFERENCES

Abel EL, Angel JM, Kiguchi K, DiGiovanni J (2009). Multi-stage chemical carcinogenesis in mouse skin: fundamentals and applications. Nat Protoc 4, 1350–1362.

Aliprantis AO, Ueki Y, Sulyanto R, Park A, Sigrist KS, Sharma SM, Ostrowski MC, Olsen BR, Glimcher LH (2008). NFATc1 in mice represses osteoprotegerin during osteoclastogenesis and dissociates systemic osteopenia from inflammation in cherubism. J Clin Invest 118, 3775–3789.

Balmain A, Ramsden M, Bowden GT, Smith J (1984). Activation of the mouse cellular Harvey-ras gene in chemically induced benign skin papillomas. Nature 307, 658–660.
Barker N, Ridgway RA, van Es JH, van de Wetering M, Begthel H, van den Born M, Danenberg E, Clarke AR, Sansom OJ, Clevers H (2009). Crypt stem cells as the cells-of-origin of intestinal cancer. Nature 457, 608–611.
Blanpain C, Lowry WE, Geoghegan A, Polak L, Fuchs E (2004). Self-renewal, multipotency, and the existence of two cell populations within an epithelial stem cell niche. Cell 118, 635–648.
Boumahdi S, Driessens G, Lapouge G, Rorive S, Nassar D, Le Mercier M, Delatte B, Caauwe A, Lenglez S, Nkusi E, *et al*. (2014). SOX2 controls tumour initiation and cancer stem-cell functions in squamous-cell carcinoma. Nature 511, 246–250.
Buchholz M, Schatz A, Wagner M, Michl P, Linhart T, Adler G, Gress TM, Ellenrieder V (2006). Overexpression of c-myc in pancreatic cancer caused by ectopic activation of NFATc1 and the Ca2+/calcineurin signaling pathway. EMBO J 25, 3714–3724.
Cotsarelis G, Sun TT, Lavker RM (1990). Label-retaining cells reside in the bulge area of pilosebaceous unit: implications for follicular stem cells, hair cycle, and skin carcinogenesis. Cell 61, 1329–1337.
Demehri S, Turkoz A, Kopan R (2009). Epidermal Notch1 loss promotes skin tumorigenesis by impacting the stromal microenvironment. Cancer Cell 16, 55–66.
de Visser KE, Eichten A, Coussens LM (2006). Paradoxical roles of the immune system during cancer development. Nat Rev Cancer 6, 24–37.
Driessens G, Beck B, Caauwe A, Simons BD, Blanpain C (2012). Defining the mode of tumour growth by clonal analysis. Nature 488, 527–530.
Euvrard S, Kanitakis J, Claudy A (2003). Skin cancers after organ transplantation. N Engl J Med 348, 1681–1691.
Goldstein J, Fletcher S, Roth E, Wu C, Chun A, Horsley V (2014). Calcineurin/Nfatc1 signaling links skin stem cell quiescence to hormonal signaling during pregnancy and lactation. Genes Dev 28, 983–994.
Hennings H, Glick AB, Greenhalgh DA, Morgan DL, Strickland JE, Tennenbaum T, Yuspa SH (1993). Critical aspects of initiation, promotion, and progression in multistage epidermal carcinogenesis. Proc Soc Exp Biol Med Soc 202, 1–8.
Horsley V, Aliprantis A, Polak L, Glimcher LH, Fuchs E (2008). NFATc1 balances quiescence and proliferation of skin stem cells. Cell 132, 299–310.
Keyes BE, Segal JP, Heller E, Lien WH, Chang CY, Guo X, Oristian DS, Zheng D, Fuchs E (2013). Nfatc1 orchestrates aging in hair follicle stem cells. Proc Natl Acad Sci USA 110, E4950–E4959.
Koenig A, Linhart T, Schlengemann K, Reutlinger K, Wegele J, Adler G, Singh G, Hofmann L, Kunsch S, Büch T (2010). NFAT-induced histone acetylation relay switch promotes c-Myc-dependent growth in pancreatic cancer cells. Gastroenterology 138, 1189–1199.e2.
Lapouge G, Youssef KK, Vokaer B, Achouri Y, Michaux C, Sotiropoulou P, Blanpain C (2011). Identifying the cellular origin of squamous skin tumors. Proc Natl Acad Sci USA 108, 7431–7436.
Li S, Park H, Trempus CS, Gordon D, Liu Y, Cotsarelis G, Morris RJ (2013). A keratin 15 containing stem cell population from the hair follicle contributes to squamous papilloma development in the mouse. Mol Carcinog 52, 751–759.
Mancini M, Toker A (2009). NFAT proteins: emerging roles in cancer progression. Nat Rev Cancer 9, 810–820.
Marafioti T, Pozzobon M, Hansmann ML, Ventura R, Pileri SA, Roberton H, Gesk S, Gaulard P, Barth TF, Du MQ, *et al*. (2005). The NFATc1 transcription factor is widely expressed in white cells and translocates from the cytoplasm to the nucleus in a subset of human lymphomas. Br J Haematol 128, 333–342.
Matsumoto Y, Ide F, Kishi R, Akutagawa T, Sakai S, Nakamura M, Ishikawa T, Fujii-Kuriyama Y, Nakatsuru Y (2007). Aryl hydrocarbon receptor plays a significant role in mediating airborne particulate-induced carcinogenesis in mice. Environ Sci Technol 41, 3775–3780.
Means AL, Xu Y, Zhao A, Ray KC, Gu G (2008). A CK19(CreERT) knockin mouse line allows for conditional DNA recombination in epithelial cells in multiple endodermal organs. Genesis 46, 318–323.
Medyouf H, Alcalde H, Berthier C, Guillemin MC, dos Santos NR, Janin A, Decaudin D, de The H, Ghysdael J (2007). Targeting calcineurin activation as a therapeutic strategy for T-cell acute lymphoblastic leukemia. Nat Med 13, 736–741.
Modi BG, Neustadter J, Binda E, Lewis J, Filler RB, Roberts SJ, Kwong BY, Reddy S, Overton JD, Galan A, *et al*. (2012). Langerhans cells facilitate epithelial DNA damage and squamous cell carcinoma. Science 335, 104–108.
Morris RJ, Liu Y, Marles L, Yang Z, Trempus C, Li S, Lin JS, Sawicki JA, Cotsarelis G (2004). Capturing and profiling adult hair follicle stem cells. Nat Biotechnol 22, 411–417.
Muller MR, Rao A (2010). NFAT, immunity and cancer: a transcription factor comes of age. Nat Rev Immunol 10, 645–656.
Muzumdar MD, Tasic B, Miyamichi K, Li L, Luo L (2007). A global double-fluorescent Cre reporter mouse. Genesis 45, 593–605.
Neal JW, Clipstone NA (2003). A constitutively active NFATc1 mutant induces a transformed phenotype in 3T3-L1 fibroblasts. J Biol Chem 278, 17246–17254.
Oikawa T, Nakamura A, Onishi N, Yamada T, Matsuo K, Saya H (2013). Acquired expression of NFATc1 downregulates E-cadherin and promotes cancer cell invasion. Cancer Res 73, 5100–5109.
Ostrand-Rosenberg S (2008). Immune surveillance: a balance between protumor and antitumor immunity. Curr Opin Genet Dev 18, 11–18.
Petersson M, Reuter K, Brylka H, Kraus A, Schettina P, Niemann C (2015). Interfering with stem cell-specific gatekeeper functions controls tumour initiation and malignant progression of skin tumours. Nat Commun 6, 5874.
Pham LV, Tamayo AT, Yoshimura LC, Lin-Lee YC, Ford RJ (2005). Constitutive NF-kappaB and NFAT activation in aggressive B-cell lymphomas synergistically activates the CD154 gene and maintains lymphoma cell survival. Blood 106, 3940–3947.
Ryeom S, Baek KH, Rioth MJ, Lynch RC, Zaslavsky A, Birsner A, Yoon SS, McKeon F (2008). Targeted deletion of the calcineurin inhibitor DSCR1 suppresses tumor growth. Cancer Cell 13, 420–431.
Sachs N, Secades P, van Hulst L, Kreft M, Song JY, Sonnenberg A (2012). Loss of integrin alpha3 prevents skin tumor formation by promoting epidermal turnover and depletion of slow-cycling cells. Proc Natl Acad Sci USA 109, 21468–21473.
Schober M, Fuchs E (2011). Tumor-initiating stem cells of squamous cell carcinomas and their control by TGF-beta and integrin/focal adhesion kinase (FAK) signaling. Proc Natl Acad Sci USA 108, 10544–10549.
Sotiropoulou PA, Candi A, Mascré G, DeClercq S, Youssef KK, Lapouge G, Dahl E, Semeraro C, Denecker G, Marine JC, *et al*. (2010). Bcl-2 and accelerated DNA repair mediates resistance of hair follicle bulge stem cells to DNA-damage-induced cell death. Nat Cell Biol 12, 572–582.
Stenn KE, Paus R (2001). Controls of hair follicle cycling. Physiol Rev 81, 449–494.
Stingl G, Koning F, Yamada H, Yokoyama WM, Tschachler E, Bluestone JA, Steiner G, Samelson LE, Lew AM, Coligan JE, *et al*. (1987). Thy-1+ dendritic epidermal cells express T3 antigen and the T-cell receptor gamma chain. Proc Natl Acad Sci USA 84, 4586–4590.
Tripathi P, Wang Y, Coussens M, Manda KR, Casey AM, Lin C, Poyo E, Pfeifer JD, Basappa N, Bates CM, *et al*. (2013). Activation of NFAT signaling establishes a tumorigenic microenvironment through cell autonomous and non-cell autonomous mechanisms. Oncogene 33, 1840–1849.
Tumbar T, Guasch G, Greco V, Blanpain C, Lowry WE, Rendl M, Fuchs E, (2004). Defining the epithelial stem cell niche in skin. Science 303, 359–363.
Vasioukhin V, Degenstein L, Wise B, Fuchs E (1999). The magical touch: genome targeting in epidermal stem cells induced by tamoxifen application to mouse skin. Proc Natl Acad Sci USA 96, 8551–8556.
Visvader JE (2011). Cells of origin in cancer. Nature 469, 314–322.
Wang J, Hu Y, Nekvindova J, Ingelman-Sundberg M, Neve EP (2010). IL-4-mediated transcriptional regulation of human CYP2E1 by two independent signaling pathways. Biochem Pharmacol 80, 1592–1600.
White AC, Khuu JK, Dang CY, Hu J, Tran KV, Liu A, Gomez S, Zhang Z, Yi R, Scumpia P, *et al*. (2014). Stem cell quiescence acts as a tumour suppressor in squamous tumours. Nat Cell Biol 16, 99–107.
White AC, Tran K, Khuu J, Dang C, Cui Y, Binder SW, Lowry WE (2011). Defining the origins of Ras/p53-mediated squamous cell carcinoma. Proc Natl Acad Sci USA 108, 7425–7430.
Wu X, Nguyen BC, Dziunycz P, Chang S, Brooks Y, Lefort K, Hofbauer GF, Dotto GP (2010). Opposing roles for calcineurin and ATF3 in squamous skin cancer. Nature 465, 368–372.
Zamarron BF, Chen W (2011). Dual roles of immune cells and their factors in cancer development and progression. Int J Biol Sci 7, 651–658.
Zito G, Saotome I, Liu Z, Ferro EG, Sun TY, Nguyen DX, Bilguvar K, Ko CJ, Greco V (2014). Spontaneous tumour regression in keratoacanthomas is driven by Wnt/retinoic acid signalling cross-talk. Nat Commun 5, 3543.
Zoumpourlis V, Solakidi S, Papathoma A, Papaevangeliou D (2003). Alterations in signal transduction pathways implicated in tumour progression during multistage mouse skin carcinogenesis. Carcinogenesis 24, 1159–1165.